Model validation using induced tensile stress during cracking process measured with desiccation stress tests

Mai Sawada[1*], *Mamoru* Mimura[2], and *Kazuhide* Yoshikawa[2]

[1]Tokyo Institute of Technology, School of Environment and Society, 1528550 Tokyo, Japan
[2]Kyoto University, Graduate School of Engineering, 6158540 Kyoto, Japan

Abstract. Tensile stress is internally induced when soil shrinkage due to desiccation is restricted, and cracks occur when the induced tensile stress reaches tensile strength. Various numerical models have been proposed to predict crack initiation; however, the validity of the computed internal stresses during the cracking process has not been assessed, although the internal stresses directly influence the crack initiation. The aim of this study was to demonstrate the effectiveness of a laboratory-based desiccation stress test, which measures the induced tensile stress until crack initiation. Desiccation stress tests were performed on unsaturated sandy soil with two different water contents. The measured tensile stress until cracking was numerically simulated using a hypo-elastic model based on the skeleton stress considering the suction effects. The computed tensile stress was consistent with the measured values throughout the cracking process in both cases, with different initial water contents. Stress-based validation using the results of the desiccation stress test demonstrated that the proposed constitutive model yields reliable estimations of the internal tensile stress in unsaturated soils until crack initiation.

1 Introduction

Desiccation cracks occur when soil shrinkage due to evaporation is restricted and the induced tensile stress reaches the tensile strength. The permeability and slope stability are significantly affected by the desiccation cracks near the ground surface. Desiccation cracks in soil cover used to protect toxic waste or tailing sites from precipitation can cause serious groundwater contamination. Therefore, in previous studies, numerical models for predicting crack initiation and propagation have been proposed using techniques that express discontinuities [1−3]. The numerical models assumed that cracks occurred when the induced tensile stress reached tensile strength. Model validations are normally carried out by comparing computed water content and time at cracking and measured values in laboratory test, which visually observe crack propagation of drying soil on petri dishes. However, the validity of the predicted internal stresses during the cracking process has not been assessed, although the internal stresses directly influence crack initiation. The accuracy of visual crack observation is another concern, because cracks can initiate earlier than they clearly appear on the soil surface.

Most constitutive models for unsaturated soils have been developed by focusing on shear failure during the wetting process to predict seepage-induced disasters; however, their applicability to tensile failure during the drying process has not been assessed. Measuring the internal stresses during the cracking process [4, 5] is useful for the development of numerical models that can accurately predict crack initiation. The aim of this study is to demonstrate the effectiveness of a laboratory-based desiccation stress test [5] that measures the tensile stress induced in a thin bar-shaped specimen with fixed ends until crack initiation. We performed desiccation stress tests on compacted unsaturated sandy soil with two initial water contents. Subsequently, the measured internal tensile stress was numerically simulated using a hypo-elastic model considering the effects of increasing suction during the cracking process to validate the proposed model.

2 Methodology

2.1 Desiccation stress test

The desiccation stress test measures the internal stress in the longitudinal direction of a bar-shaped specimen until crack initiation, by measuring the strain of an embedded aluminum plate. Fig. 1 shows the specimen and the aluminum plate used for the desiccation stress test. Decomposed granite soil was passed through a 2-mm sieve (sand: 58.0%, silt: 17.3%, clay: 24.8%) with an initial water content of 23 or 29%. The specimen shown in Fig. 1 (a) was prepared by tamping the soil at a dry density of 1.37 g/cm^3 in a mold, which was lined with greased Teflon sheets for smooth removal of the specimen. The specimen was prepared by dividing the upper and lower halves to reduce density variation in the depth direction. An aluminum plate (length: 200 mm, width: 10 mm, thickness: 1 mm) was placed on the

* Corresponding author: sawada.m.af@m.titech.ac.jp

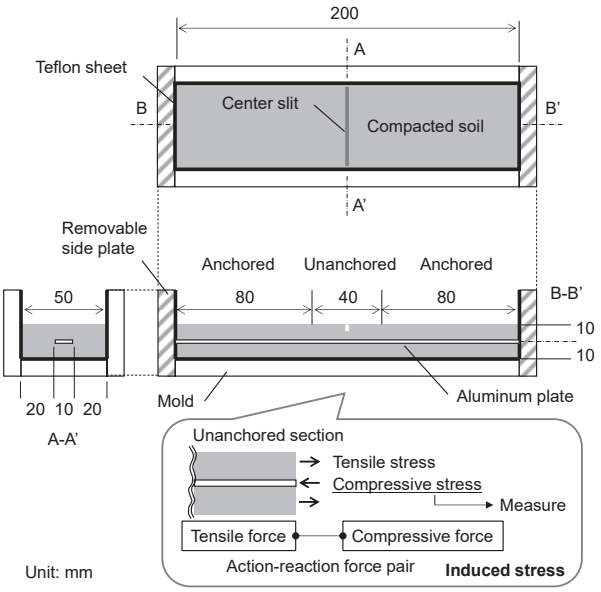

(a) Specimen

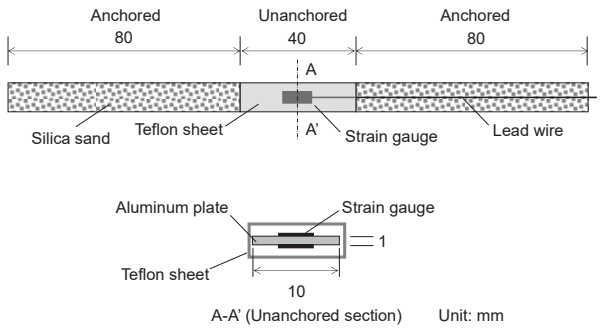

(b) Aluminium plate with strain gauges

Fig.1. Desiccation stress test

surface of the lower layer. The lower layer surface was scored with a sharp stick to avoid discontinuity between the lower and upper layers.

The role of the anchored sections of the aluminum plate shown in Fig. 1 (b) was to restrain desiccation shrinkage and induce a crack in the unanchored section. The surface roughness of the aluminum plate in the anchored sections was increased by attaching air-dried silica sand to both faces with double-sided adhesive tape to enhance the cohesion between the aluminum plate and the specimen. The unanchored middle section of the aluminum plate was covered with a lubricated Teflon sheet, and strain gauges were attached to both faces to measure the compression strain that occurred when the specimen shrinkage was restricted. The compression forces exerted on the aluminum plate were estimated by multiplying the measured strain by Young's modulus (i.e., 60,475 MN/m^2), which equals the internal tensile force generated in the soil in magnitude based on the law of action-reaction.

The specimen with the Teflon liner was carefully removed from the mold and a surface slit was introduced to induce a crack at the center of the specimen. The test was performed in a constant climate chamber at a temperature of 20 °C and a relative humidity of 60% RH, based on the vapor pressure method. The specimens were placed on an electric scale to calculate the water content by using the measured specimen mass during the cracking process. The strains of the aluminum plate and mass of the specimen were recorded at intervals of 1 min until a crack occurred at the center slit. Thirteen specimens with initial water contents of 23 and 29% were tested. Further details of the desiccation stress test have been provided in the literature [5].

2.2 Modeling internal tensile stress during cracking process

Variations in deformation moduli and volume due to increasing suction in drying soil should be considered in constitutive models for expressing desiccation cracking. Jommi et al. (2016) [6] expressed the induced tensile stress of clayey soil during the cracking process using a hypo-elastic model, assuming that the soil saturation was maintained and its volumetric change was equal to the evaporation. The effective stress was defined as the sum of the total stress and suction based on Terzaghi's effective stress, which extended to the negative porewater pressure. In the present study, the constitutive model was modified for application to unsaturated soils.

The hypo-elastic model assumed here describes the soil stiffness as follows:

$$\begin{bmatrix} \dot{p'} \\ \dot{q} \end{bmatrix} = \begin{bmatrix} K & 0 \\ 0 & 3G \end{bmatrix} \begin{bmatrix} \dot{\varepsilon_{vol}} \\ \dot{\varepsilon_d} \end{bmatrix} \quad (1)$$

$$p' = (2\sigma'_{LV} + \sigma'_{LO})/3 \quad (2)$$

$$q = \sigma'_{LV} - \sigma'_{LO} \quad (3)$$

$$\varepsilon_{vol} = 2\varepsilon_{LV} + \varepsilon_{LO} \quad (4)$$

$$\varepsilon_d = 2(\varepsilon_{LV} - \varepsilon_{LO})/3 \quad (5)$$

where K is the tangent bulk modulus, and G is the shear modulus. The stress and strain in the lateral and vertical directions of the specimen used for the desiccation stress test were assumed isotropic. The index LV represents the lateral and vertical directions and LO represents the longitudinal direction. Stress is expressed by Eq. (6), referred to as skeleton stress [7, 8], which corresponds to Bishop's effective stress when its parameter χ, is defined as the degree of saturation S_r. The term, $u_a - u_w$, represents the matric suction. The skeleton stress, expressed by Eq. (6) is equivalent to the effective stress defined in the original model [6] when S_r = 1. Under the boundary condition of $\dot{\varepsilon_{LO}} = 0$, the longitudinal skeleton stress increment is expressed by Eq. (7).

$$\sigma' = \sigma - u_a + S_r \cdot (u_a - u_w) \quad (6)$$

$$\dot{\sigma_{LO}} = \dot{p'} - 2G\dot{\varepsilon_{vol}}/3 \quad (7)$$

The longitudinal total stress increment is expressed as follows when mean total stress is constant (i.e., $\dot{p} = 0$):

$$\dot{p'} = \dot{p} + \dot{s} = \dot{s} \quad (8)$$

$$s = S_r \cdot (u_a - u_w) \quad (9)$$

$$\dot{\sigma_{LO}} = \dot{\sigma_{LO}} - \dot{s} = -2G\dot{\varepsilon_{vol}}/3 \quad (10)$$

Eq. (10) can be rewritten using Poisson's ratio ν as follows:

$$\dot{\sigma_{LO}} = -\frac{1-2\nu}{1+\nu} K\dot{\varepsilon_{vol}} = -\frac{1-2\nu}{1+\nu}\dot{s} \quad (11)$$

The desiccation stress test measures longitudinal total stress, σ_{LO}. The numerically estimated values using Eq. (11) were compared with the measured values to validate the constitutive model.

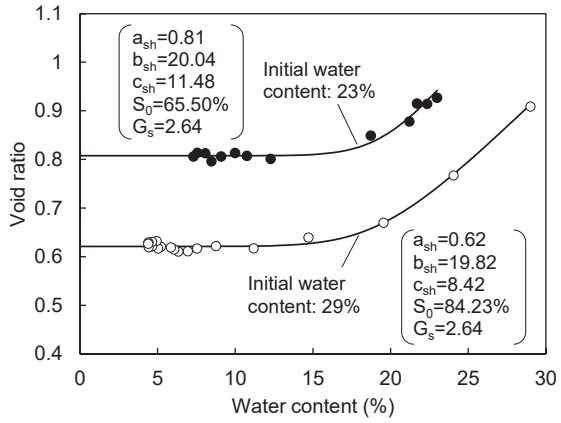

Fig.2. Shrinkage curves

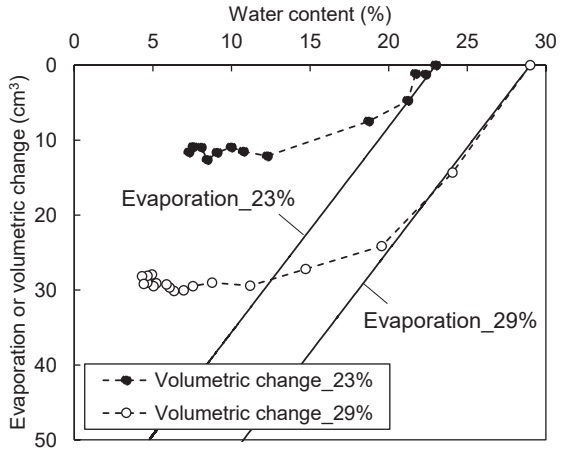

Fig.3. Evaporation and volumetric change

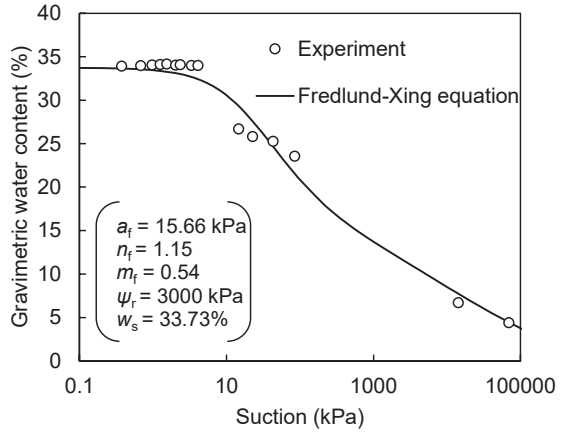

Fig.4. w-SWCC

The stress induced by suction s, was calculated using the experimentally obtained shrinkage curves and a soil water characteristic curve based on the gravimetric water content (w-SWCC). Fig. 2 shows the shrinkage curves for the tested soil with different initial water contents, which were fitted to a mathematical equation [9]. The shrinkage curves were obtained using the measured volumetric changes and evaporation as shown in Fig. 3. The specimens were prepared in the same manner as for DST, but without the installation of the aluminium plates, and dried under constant climatic conditions of 20 °C and 60% RH. The volume of the specimen was obtained by taking a photo every 3 h using a camera set above the specimen, and reading the length and width from the photos using AutoCAD. The shrinkage curves indicate that the volumetric change becomes less than the evaporation as the soil dries. Thus, the assumption used to estimate the volumetric change in the original model proposed by Jommi et al. (2016) cannot be applied to unsaturated tested soils. Thus, the modified model employed shrinkage curves to estimate the volumetric change induced by the applied suction. Essentially, S_r was estimated using the void ratio based on the shrinkage curves, and substituted to Eq. (9) to obtain s. The increment of s is equivalent to that of longitudinal total stress, σ_{LO} as shown in Eq. (11).The w-SWCC shown in Fig. 4 was obtained by a water retention test and fitted to the Fredlund-Xing equation [10], which is applicable to a wide range of suction. The model parameters used for the shrinkage curves and w-SWCC are presented in the figures.

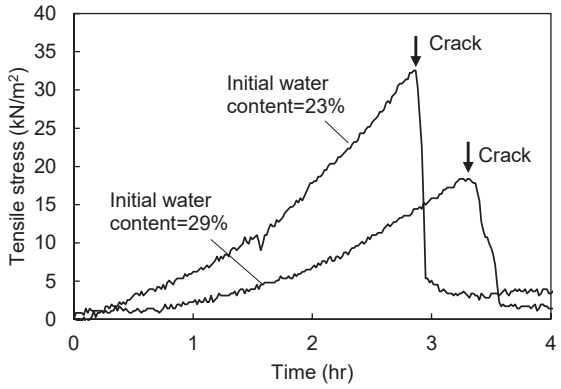

Fig.5. Measured tensile stress

3 Results and discussions

3.1 Experimental results

Fig. 5 shows the induced tensile stress of the two specimens with different initial water contents measured using the desiccation stress test (DST). The tensile stress increased several hours from the start until a crack was initiated and dropped sharply as the crack opened. Crack initiation was detected via stress measurement until the crack became clearly visible on the specimen surface, which is a significant advantage of the desiccation stress test.

The measured values at cracking are presented in Table. 1. The degree of saturation at cracking was estimated using the shrinkage curve. The measured peak tensile stress varied, although 13 specimens with the same initial water content were tested under the same conditions. This can be attributed to the characteristics of tensile failure, which is sensitive to specimen

Table. 1 Measured values at cracking

(a) Initial water content: 29%

No.	Time (hr)	Water content (%)	Void ratio	Degree of saturation (%)	Tensile stress (kN/m^2)
29-1	3.32	23.67	0.76	82.23	18.38
29-2	4.33	24.16	0.77	82.52	20.64
29-3	2.50	24.84	0.79	82.85	18.67
29-4	3.00	23.31	0.75	81.99	15.84
29-5	3.00	25.68	0.82	83.17	6.22
29-6	2.83	24.39	0.78	82.64	5.94
29-7	2.67	24.12	0.77	82.50	10.75
29-8	3.50	23.07	0.74	81.80	20.93
29-9	2.83	24.39	0.78	82.64	5.94
29-10	3.00	24.15	0.77	82.51	13.07
29-11	3.05	23.75	0.76	82.28	11.88
29-12	3.73	23.86	0.77	82.35	18.95
29-13	4.30	23.56	0.76	82.16	15.55
Max	4.33	25.68	0.82	83.17	20.93
Min	2.50	23.07	0.74	81.80	5.94
Mean value	3.24	24.07	0.77	82.43	14.06
Standard variation	0.56	0.65	0.02	0.35	5.33

(b) Initial water content: 23%

No.	Time (hr)	Water content (%)	Void ratio	Degree of saturation (%)	Tensile stress (kN/m^2)
23-1	3.40	17.88	0.82	57.22	20.08
23-2	2.30	19.99	0.86	61.58	16.69
23-3	1.92	21.12	0.88	63.05	12.16
23-4	2.15	20.26	0.86	61.98	15.27
23-5	3.60	18.79	0.84	59.36	29.41
23-6	2.15	19.36	0.84	60.50	19.70
23-7	0.90	21.31	0.89	63.25	9.62
23-8	3.88	17.53	0.82	56.33	33.94
23-9	2.43	18.63	0.83	59.01	24.04
23-10	3.97	17.44	0.82	56.08	32.24
23-11	2.33	19.63	0.85	60.98	18.38
23-12	4.83	16.66	0.82	53.91	46.95
23-13	2.85	18.38	0.83	58.44	32.52
Max	4.83	21.31	0.89	63.25	46.95
Min	0.90	16.66	0.82	53.91	9.62
Mean value	2.82	19.00	0.84	59.36	23.92
Standard variation	1.02	1.38	0.02	2.77	10.14

variation due to minor deficiencies, as a similar tendency is commonly observed in tensile tests.

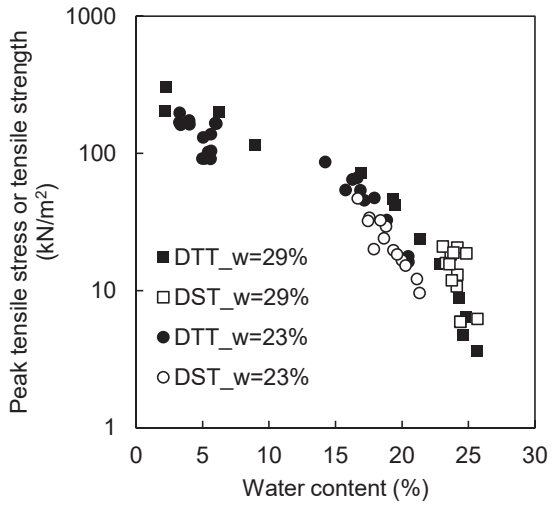

Fig.6. Peak tensile stress and tensile strength

The peak tensile stress values were compared with the tensile strength measured by direct tension test (DTT) [5] to assess the validity of the tensile stress measured with DST. The specimens used for DTT were prepared in the same manner as those used for DST, but without the installation of the aluminum plate, and dried under constant climatic conditions of 20 °C and 60% RH. Fig. 6 shows the relationships between the peak tensile stress and water content at cracking measured with DST and the tensile strength–water content relationships obtained with DTT. The relationships obtained with DST almost overlapped with those obtained with DTT, which shows that cracks initiated when the induced tensile stress reached tensile strength. These results indicate that the DST yielded reasonable tensile stress measurements until crack initiation.

3.2 Numerical simulation

The induced tensile stress in the longitudinal direction measured by the desiccation stress test was numerically simulated using the constitutive model described in Section 2.2. The shrinkage curves, w-SWCC, and

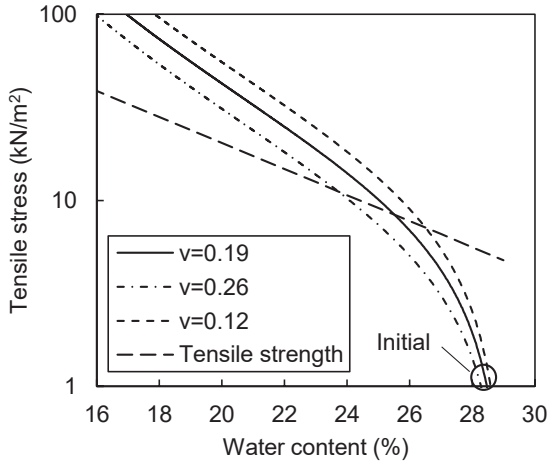

(a) Initial water content: 29%

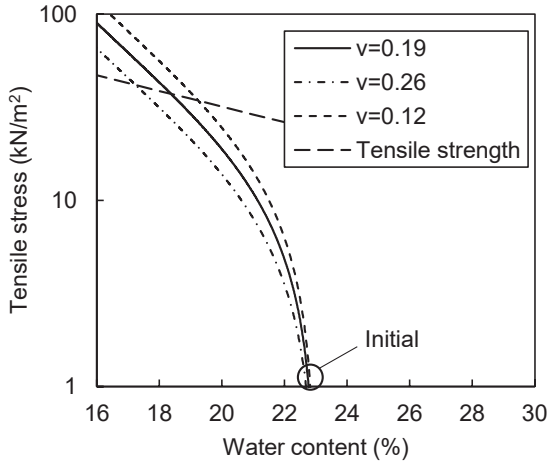

(b) Initial water content: 23%

Fig.7. Computed tensile stress

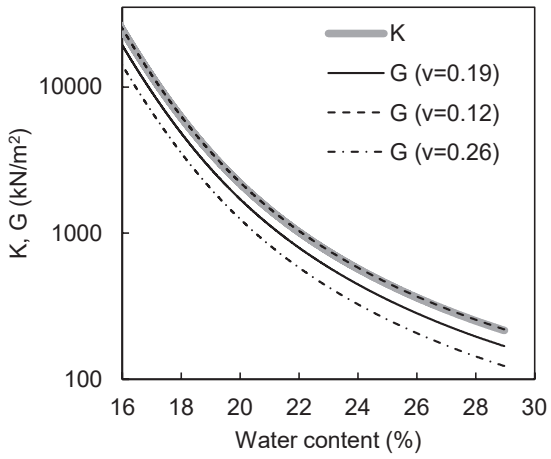

(a) Initial water content: 29%

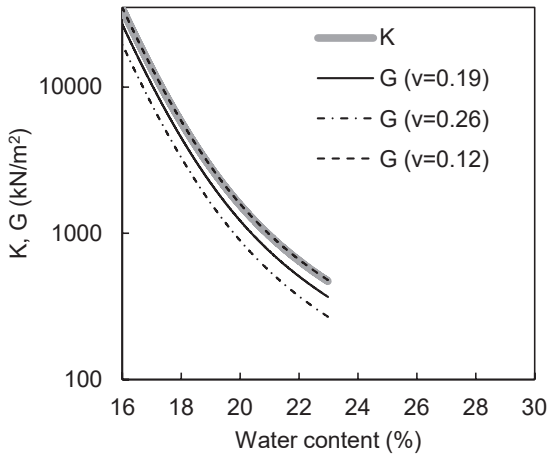

(b) Initial water content: 23%

Fig.8. Estimated deformation moduli

Poisson's ratio are necessary to estimate σ_{LO}, as shown in Eq. (11). Here, Poisson's ratio was estimated to be 0.12–0.26, based on the results of triaxial tests under constant suction of 0 to 80 kPa, showing that it was almost constant within the range of suction, and the mean value was 0.19 with a standard deviation of 0.07 [5]. The induced tensile stress–water content relationship is computed using Eq. (11) when suction was increased at an interval of 0.1 kPa, are shown in Fig. 7. An approximated tensile strength–water content curve based on the results of the direct tension test (Fig. 6), which corresponds to a failure envelope, is shown in the figure. Cracks were predicted to occur in specimens with a certain initial water content at the intersections of the tensile stress curves and failure envelope.

Fig. 8 shows the estimated tangent bulk modulus or shear modulus–water content relationship. The tangent bulk modulus increased with an increase in the mean skeleton stress p'. Here, $\dot{p}'$ is equal to the increment of $\dot{s}$, the stress induced by suction. Shear modulus, which is related to the tangent bulk modulus, shows a similar tendency as the tangent bulk modulus, but it varies depending on Poisson's ratio. The variations in the deformation moduli during the cracking process indicate that the specimen became stiff as the intergranular stresses induced by suction increased. Therefore, the induced tensile stress exponentially increases throughout the cracking process, as shown in Fig. 7, although shrinkage slows as the specimen dries, as shown in Fig. 2. The tensile strength and stiffness of the specimen increased as suction developed, as shown in Fig. 6. Essentially, both the tensile strength and induced tensile stress increase as the specimen dries, and a crack occurs when the induced tensile stress reaches the tensile strength. At the start of the test, the internal stress in the specimen was zero regardless of the initial water content of the specimen, whereas the tensile strength was higher when the initial water content was lower. Thus, the tensile stress at cracking was higher when the initial water content was lower, as shown in Fig. 7.

Fig. 9 shows comparisons between the computed and measured induced tensile stress–water content relationships. In both cases with different initial water content, most of the measured curves were consistent with the computed curves. This shows that skeleton stress defined as Eq. (6) can appropriately estimate suction contribution in tensile failure during the drying process, as well as that in shear failure during wetting process [7, 8]. The discrepancies between the measured and computed tensile stress is slightly larger when initial

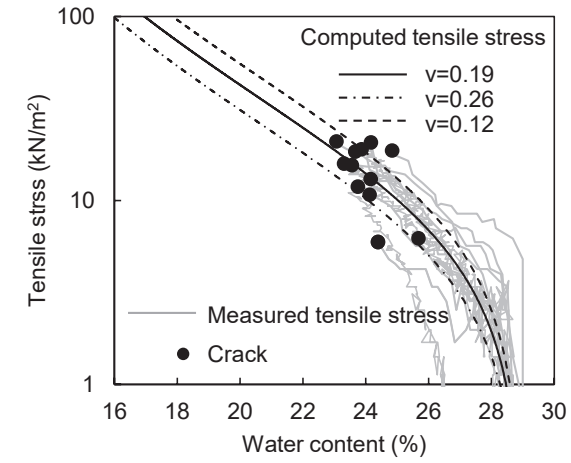

(a) Initial water content: 29%

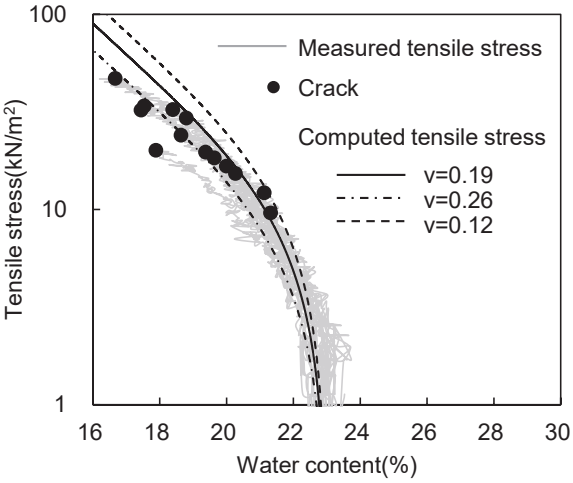

(b) Initial water content: 23%

Fig.9. Measured and computed tensile stresses

water content is lower. This can be attributed to a difference in SWCCs between initially unsaturated and saturated specimens. The SWCCs of the unsaturated specimens for DST can have lower suction at a certain water content than that of the main drying curve shown in Fig. 4, which was obtained using an initially saturated specimen. Although further study is needed on SWCCs in DST to compute tensile stress more accurately, the proposed constitutive model yields reliable estimations of internal tensile stress in unsaturated soils until crack initiation. Numerical simulation used to be the only way of estimating the internal stress during cracking process, and its validation was limited at cracking when tensile stress equals to measurable tensile strength [1−3]. The desiccation stress test measures only one-dimensional internal stress when a single crack occurs, and the measured stress is not valid anymore after crack initiates, however it enables stress-based model validation from the start to until crack initiation.

4 Conclusions

This study demonstrated the effectiveness of the desiccation stress test, which measures the induced internal stress in the soil during desiccation cracking, in developing constitutive models for predicting desiccation cracking. Desiccation stress tests were performed on specimens with two different initial water contents, and the induced tensile stress was measured until crack initiation. The experimental results were used to validate the numerically predicted tensile stress based on a constitutive model that considered the effects of suction during the cracking process.

The measured tensile stress at cracking was consistent with the tensile strength measured by the direct tension test, indicating that the desiccation stress test yielded quantitatively reliable tensile stress measurements until crack initiation. A hypo-elastic model based on skeleton stress considering the suction contribution to intergranular stresses in unsaturated soil was applied to simulate the tensile stress measured with the desiccation stress test. The computed tensile stresses were consistent with the measured values regardless of the initial water content of the specimens, which showed that skeleton stress can appropriately estimate the suction contribution in tensile failure during the drying process, as well as that in shear failure during the wetting process. The stress-based validation using the results of the desiccation stress test demonstrated that the proposed constitutive model yields reliable estimations of the internal tensile stress in unsaturated soils from the start to crack initiation.

Acknowledgements

This work was supported by JSPS KAKENHI (grant number 18K13827).

References

1. R. Rodríguez, M. Sánchez, A. Ledesma, A. Lloret. Can. Geotech. J. **44**, 6, 644-658 (2007)
2. H. Trabelsi, M. Jamei, H. Zenzri, S. Olivella, (2012). Int J Numer Anal Methods Geomech, **36**, 11, 1410-1433 (2012)
3. M. Sánchez, O.L. Manzoli, L.J. Guimarães. Comput. Geotech. **62**, 27–39 (2014)
4. M. Varsei, G.A. Miller, A. Hassanikhah. Int J Geomech, **16**, 6 (2016)
5. M. Sawada, Y. Sumi, M. Mimura. Soils Found. **61**, 4, 915-928 (2021)
6. C. Jommi, N. Valimberti, R.N. Tollenaar, G. Della Vecchia, L.A. van Paassen. E3S Web of Conferences. **9** (2016)
7. C. Jommi. Experimental evidence and theoretical approaches in unsaturated soils, 147-162 (2000)
8. D. Gallipoli, A. Gens, R. Sharma, J. Vaunat. Géotechnique, **53**(1), 123-135 (2003)
9. M.D. Fredlund, G.W. Wilson, D.G. Fredlund. Proc. 3rd International Conference on Unsaturated Soils, 145-149 (2002)
10. D.G. Fredlund, A. Xing. Can. Geotech. J. **31**, 4, 521-532 (1994)